CONF-960401--36 SAND96-1279C

PREPARATION OF MICROPOROUS FILMS WITH SUB NANOMETER PORES AND THEIR CHARACTERIZATION USING STRESS AND FTIR MEASUREMENTS

J. Samuel*, A. J. Hurd*, F. van Swol††, L. J. Douglas Frink††, C.J. Brinker*†, S.C. Contakes*; Ceramic Processing Science Department, Sandia National Laboratories, Albuquerque, NM 87185-0609*; Department 9225, Sandia National Laboratories, Albuquerque, NM 87185-1111††, UNM-NSF Center for Micro engineered Ceramics, University of New Mexico, Albuquerque, NM 87131†

ABSTRACT

We have used a novel technique, measurement of stress isotherms in microporous thin films, as a means of characterizing porosity. The stress measurement was carried out by applying sol-gel thin films on a thin silicon substrate and monitoring the curvature of the substrate under a controlled atmosphere of various vapors. The magnitude of macroscopic bending stress developed in microporous films depends on the relative pressure and molar volume of the adsorbate and reaches a value of 180 MPa for a relative vapor pressure, P/Po = 0.001, of methanol. By using a series of molecules, and observing both the magnitude and the kinetics of stress development while changing the relative pressure, we have determined the pore size of microporous thin films. FTIR measurements were used to acquire adsorption isotherms and to compare pore emptying to stress development. about 80% of the change in stress takes place with no measurable change in the amount adsorbed. We show that for sol-gel films, pore diameters can be controlled in the range of 5 - 8 Å by "solvent templating".

INTRODUCTION

The formation of porous thin films with precisely controlled pore size in the microporous range, and the characterization of porosity in this range are of interest for their potential use as membrane materials[1] and in selective sensor applications[2].

The determination of pore size and pore size distribution in microporous materials by means of adsorption isotherms becomes fraught with complications as pores become smaller[3], the usual cutoff is considered to be at a pore diameter of 20Å. These complications arise because the Kelvin equation no longer predicts the capillary filling of micropores in which surface adsorbate interactions become overwhelming.

One approach to the determination of pore size, or constriction size, in microporous materials is the measurement of sieving behavior of the adsorbent towards a series of molecules of increasing size. This approach has been used in bulk materials such as microporous carbons[4].

In thin films, with a thickness on the order of 1000Å-2000Å, the inherent ambiguity in the analysis of the adsorption isotherm is further compounded by technical difficulty in acquiring an adsorption isotherm in which only nanograms of material are adsorbed. Highly sensitive microbalance techniques, such as the surface acoustic wave technique, have been used to acquire adsorption isotherms of mesoporous materials[5]. In microporous materials, appreciable solvation stress associated with the change in relative pressure has been seen to overwhelm the effect of adsorbed mass[6]. An interesting approach has been the use of ellipsometry to determine the pore size of several sol gel films by observing the change in index of refraction on adsorption of a series of molecules[7].

We have used a beam bending technique[8] to measure the change in solvation stress in a thin film as a result of adsorption[9]. The method employs the measurement of both the kinetics and the magnitude of change in stress induced in a porous film as a result of changing the overlying relative vapor pressure, P/P_0. Using a homologous series of molecules, the molecular sieving properties of several silica films formed by the sol-gel method were characterized.

A major goal in the area of porous materials is the manipulation of pore size. Employing the aforementioned technique as a method of characterization, we have observed that the porosity in acid catalyzed sol-gel thin films is templated by the solvent from which the film is deposited. On increasing the alcohol size from which the film is deposited, from methanol up to cyclohexanol, we observed a concomitant increase in the average pore size.

EXPERIMENTAL

Sol preparation and deposition: A2 sols: Sols were prepared from tetraethoxysilane (TEOS), water and HCl in a two step process. In the first step, a stirred solution of TEOS was partially hydrolyzed under reflux for 90 minutes (TEOS: ethanol: water: HCl ratio of 1: 3.8: 1: 7x10-4). In the second step water, ethanol and acid were added to give a final TEOS: ethanol : water : HCl : Ratio of 1:19.6 : 5.1 : 0.056. The films were deposited on 150μm or 75μm thick <100> double polished silicon wafers by dipcoating in a dry atmosphere ([H20]~10ppm) at a speed of 1.7 mm/sec. The films were deposited on one side of the wafer by masking the opposite side with a layer of parafilm which was removed before heating the films to a temperature of 400 °C. The film thickness, measured by ellipsometry, was ~1000 Å. P-25 films were prepared by using 25 mole% of phenyltriethoxysilane (PTES) in the first step and calcining the deposited film at 575 °C for 30 minutes.

Solvent exchanged A2 sols: Prior to solvent substitution A2 sols were aged for 10.5 hours (t/tg = 0.25). 25 mL of sol was diluted with 3 volumes of the solvent to be exchanged. The sol was placed in a rotary evaporator under vacuum applied by an oil pump and evaporated down to a volume of 25 mL. This process was repeated 5 times for ethanol, 2-propanol, tert butanol and cyclohexanol and repeated 7 times for methanol.

Stress Measurement: The stress measurement was carried out using a beam bending or cantilever technique[8], [9]. The thin porous film is deposited on a substrate (beam) of known thickness and modulus and the amount of stress exerted by the film is found from the change in curvature of the beam. The thin films were deposited on one side of 150μ or 75μ <100> single crystal double polished silicon wafers. A sample with dimensions of approximately 1 cm width and 5 cm length was clamped in a vertical position in the vacuum chamber. The sample was pumped down to a pressure of 10^{-5} torr. Pressure is measured with a series of stabilized MKS transducers (0.1, 10 and 100 torr full scale). A 6mw HeNe laser is passed through a x40 beam expander and iris to reduce divergence and is then bounced off the uncoated side of the sample. The beam is bounced between 4 mirrors and is detected at a position sensitive detector (UDT model SL15). The path length of the beam can be changed to accommodate different extents of deflection. The solvent, after being degassed by freeze thaw cycles, is dosed into the chamber through a needle valve. The dosing is automatically controlled and the pressure and height of the reflected laser spot are stored in the computer after a predetermined equilibration time. The stress measurement may be run in a kinetic mode by abruptly changing the partial pressure over the sample and following the stress at 1 second intervals, or an isotherm may be automatically collected for a series of pressures.

The lateral deflection of the wafer, δ, at the point that the laser hits the sample, is related to the change in height of the laser spot on the detector, h, by $\delta = L\,h\,/(4P)$ where P is the path length from the sample to detector, and L is the cantilever length. Under conditions of small deflection and film thickness relative to substrate thickness, δ is related to the stress in the film, s, by Stoney's equation[9]: $s = E_w\,d_w^2\,/\,(3L^2\,(1-\nu_w)\,d_f)\,\delta$ where E_w is Young's modulus of the substrate, d_w is the substrate thickness, d_f is the film thickness and ν_w is the substrate Poisson ratio.

Van der Waals diameters of the probe molecules, σ, were estimated using Biosym™ molecular modeling program by calculating the smallest diagonal of a square that could fit around the molecule.

IR measurements. Infrared adsorption spectra were collected on a Nicolet 800 FTIR equipped with a vacuum cell. Spectroscopic determination gave us sufficient sensitivity to measure the small amounts adsorbed on the thin film (up to 0.84 μgrams/cm^2 at saturation). The sample under vacuum was used as a background and the spectra from 975 cm-1 to 4000 cm-1 were collected under controlled vapor pressure. The spectra were corrected for the vapor phase contribution using an uncoated wafer at similar pressures.

RESULTS AND DISCUSSION.

Stress Kinetics: With saturation taken as the zero stress reference point, stress in the film becomes increasingly tensile as the relative pressure is reduced. The absolute change in stress

observed between saturation and vacuum reaches 220MPa. for an A2 film under methanol (Figure2).

The kinetics of the change in stress observed by abruptly changing the overlying vapor pressure, becomes slower as the size of the probe molecule approaches the size of the pores or limiting constrictions. In the case of the standard A2 sample, the kinetics of stress change on adsorption of methanol (σ = 5.6 Å) , acetonitrile (σ = 5.5 Å) and water are on the order of seconds, not resolvable in our system. Ethanol (σ = 6.2 Å) shows much slower kinetics (Figure 1A), quasi-exponential with a half life of 180 minutes and a smaller overall change in stress, 60 MPa versus 220 MPa for methanol. On dosing in 2-propanol (σ = 7.6 Å), no change in the state of stress is discernible. The much slower kinetics on going from methanol to ethanol, and the absence of any discernible change in stress when dosed with 2-propanol indicates that the pore size falls between that of methanol and 2-propanol largely centered around ethanol.

In the case of a film prepared with 25% PTES (P-25 film), in which the phenyl groups are subsequently calcined under reducing conditions, the kinetics of stress change on adsorption shows a small reduction in rate for tert-butanol (σ = 8.1 Å), Figure 1B, compared to smaller alcohols. On dosing with cyclohexanol, (σ = 8.6 Å), an appreciable reduction in the rate, and a drop in the overall magnitude of stress change from ~100 Mpa. to 40 Mpa takes place. The reduction in the magnitude of induced stress, observed as the molecule size is increased, may be attributed to the fact that the larger molecule is excluded from a large part of the pore volume and hence can not induce a change in stress.

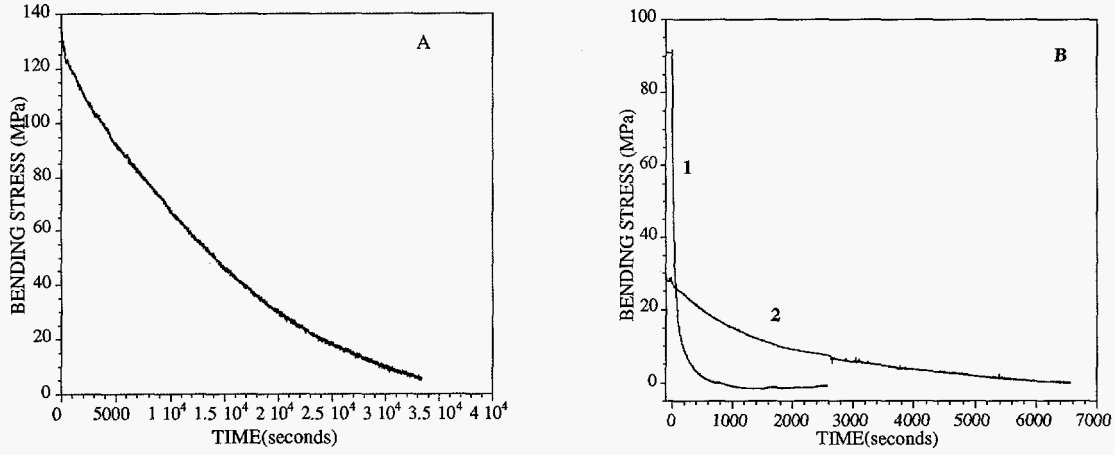

Figure 1 Kinetics of stress change on adsorption of alcohols. **A** : A2 film on dosing in ethanol, this compares with a change of seconds, limited by instrument response for methanol, acetonitrile and water. **B** P-25 film, the faster kinetics (1) is observed on dosing in 2-propoanol, the slower kinetics (2) is seen on dosing in cyclohexanol.

Isotherms: For the microporous acid catalyzed films, the stress isotherms for various adsorbates show a monotonic change in stress as the relative pressure P/P_0 is reduced (Figure 2). With the saturated state taken as the unstressed state then the tension may be displayed as increasing as the relative presure is reduced. The initial part of the curve is linear in $\ln(P/P_0)$ and the ratio of the slopes, for different adsorbates on the same sample, is equal to the inverse ratio of the bulk molar volumes of the adsorbates

Adsorption isotherms measured by FTIR for the same film show a sharp type 1 isotherm typical of microporous materials as may be seen in Figure 2B. The normalized amount adsorbed, plotted in the isotherm, is found from the peak area of 3600-2750 cm^{-1}. This encompasses a broad OH stretch band centered at 3330 cm-1 and CH_3 stretches at 2956.8 cm^{-1} and 2848.6 cm^{-1}.The most noteworthy feature of the adsorption and stress isotherms, that is clearly noticeable when they are juxtaposed, is that the bulk of the stress change takes place with no appreciable change in the

amount adsorbed, i.e. while the pores are saturated, (Figure 2A). This indicates that the stress induced is not a result of swelling simply due to an increase in the amount adsorbed.

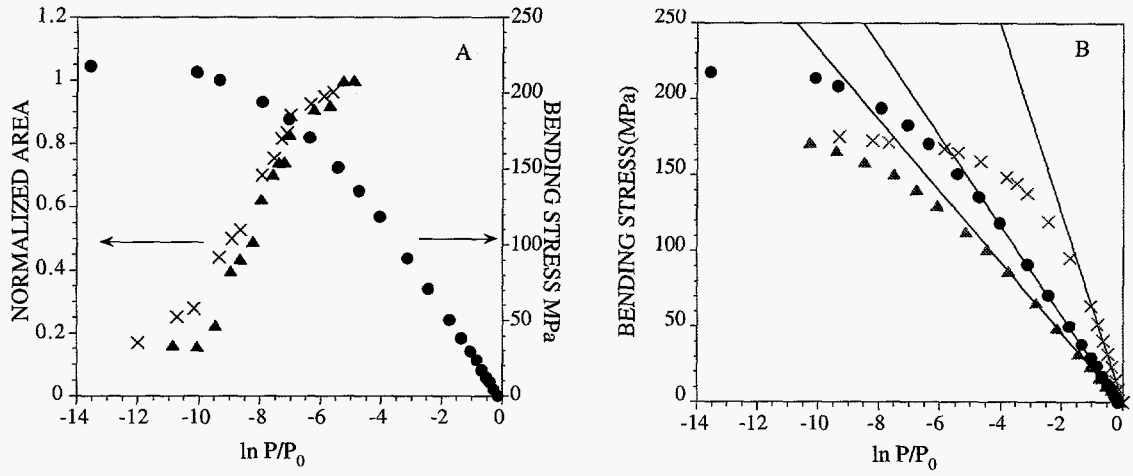

Figure 2: Adsorption and stress isotherms for an A2 film. **A:** Adsorption isotherm for methanol measured by FTIR (left axis) and stress isotherm (right axis); ▲ adsorption, x desorption, stress ● adsorption. **B** stress isotherm for: ▲ acetonitrile, ● methanol, x water. The straight lines are the best fit to the initial, linear part of the curves.

Capillary condensation under reduced relative pressure induces tensile stress[10]. For large enough pores, the Kelvin and Laplace equations yield the following equation[11]

$$s_{bend} \propto P_c = \gamma/r_m = -\ln(P/P_o)\, R_g T/V_m \qquad (1)$$

essentially this equation is a chemical potential equation, with the capillary stress P_c following the chemical potential. Comparing equation 1 to the experimental results we see that the ratio of the slopes for various solvents, on the same film, should be equal to the inverse ratio of the molar volumes, as is indeed observed experimentally.

What we measure in the experiment is the bending stress s_{bend}, this is related to the solvation induced stress by equation 2[12]:

$$s_{bend} = C_\upsilon \zeta P_c \qquad (2)$$

where υ is Poisson's ratio and $C_\upsilon = (1-2\upsilon)/(1-\upsilon)$[13]. C_υ stems from the biaxial nature of the stress developed due to attachment of the film to the substrate. For a typical value of $\upsilon = 0.2$ measured for a variety of silica gels, $C_\upsilon = 0.75$[13]. The parameter ζ for a saturated porous media is generally accepted to be $1-(K_n/K_S)$ [14] where K_n is the bulk modulus of the film and K_S is the bulk modulus of the silica skeleton. As the porosity of a film increases K_n drops and $\zeta \rightarrow 1$. Assuming $C_\upsilon = 0.75$, for the A2 film, with the lower porosity, $\zeta = 0.65$ while for the more porous P-25 film, $\zeta = 0.92$.

Although the explanation of the experimental results in the framework of capillary tension is beguiling in its simplicity, there are difficulties that arise on closer examination. It is clear from surface force apparatus experiments that the characteristics of fluids confined in small dimensions differ greatly from bulk fluid characteristics[15]. Indeed, the density and solvation force of a fluid confined between to plates is seen to oscillate widely as a result of packing constraints. While the slope found experimentally is consistent with Equation 1, the magnitude of the tensile stress that is induced in the fluid is considerably beyond the predicted tensile strength of the bulk

liquid[16],[11]. An additional point, is that for a system in which the stress is a result of the tensile state of the liquid at reduced P/P_0, one would expect the stress to disappear when the pores emptied, so that a maximum in tensile stress would be observed at the point that the pores begin to empty. For microporous materials we see a monotonic change in stress with decreasing P/P_0.

Theoretical work done recently by F. van Swol and L.J. Douglas Frink, using a density functional approach, indicates that in the limit of small pores, with a pore diameter($2r_p$) / solvent diameter (σ) ratio of up to approximately 4, in which there is a limited amount of polydispersity, the state of the adsorbed fluid at saturation will be compressive. The stress is predicted to drop on reducing P/P_0 with a slope of $ds/d\ln(P/P_0) = R_gT/V_m$, the same slope as that predicted in equation 1. While $ds/d\ln(P/P_0)$ oscillates as a function of r_p/σ for a monodisperse pore, these oscillations are smoothed out for a polydisperse system. As the oscillations of the derivative are around R_gT/V_m, averaging out around the oscillations as a result of a distribution of pores leads to the same slope predicted by the Kelvin equation. A Gaussian distribution with a standard deviation of 0.3-0.5 σ is consistent with the experimental results. The stress goes from compressive at saturation, to zero under vacuum and is predicted to drop monotonicly with $\ln P/P_0$ as is observed in the experiment. As the initial stress is compressive there is no inherent limitation on the difference in stress between the saturated state and the in vacuo state.

SOLVENT TEMPLATING: In the previous section we observed that the standard A2 films deposited from ethanol have a final pore size, or constriction size, around the size of an ethanol molecule. This indicates a possible method of manipulating pore size by solvent templating. The sol-gel film formed during dipcoating may collapse around residual solvent molecules and these template, at least roughly, the pores. In order to check this, we prepared solvent exchanged sols, using a series of alcohols. After depositing the films from the various alcohols and calcining, the stress induced in films was measured on adsorbing the same series of alcohols. As can be seen in figure 3, The maximum stress in each film is observed at the point at which the probe molecule is the same as the solvent from which the film was deposited.

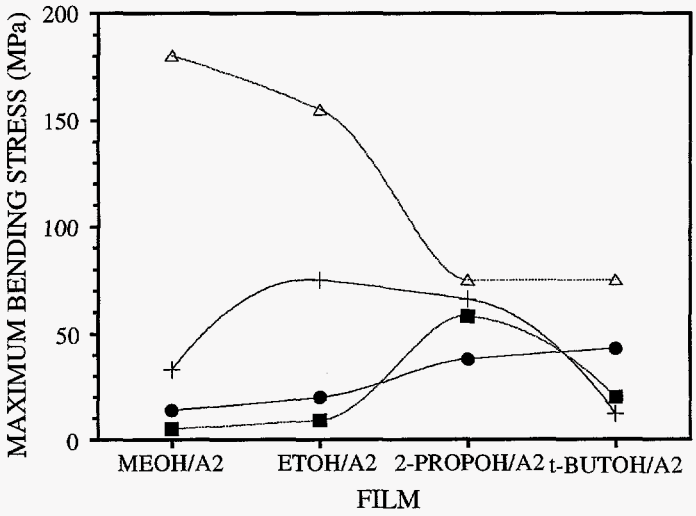

Figure 3: Maximum stress induced in solvent templated films by Δ methanol, + ethanol, ■ 2-propanol and ● t-butanol

When the average pore size is smaller than the probe size, only part of the volume of the porous network is accessible and the magnitude of the stress induced on saturation is reduced. On the other hand, when the average pore size is greater than the probe size, the stress observed will increase as the average pore size approaches the probe size. This increase comes about because the stress increases for a smaller r_p/σ and for a narrower distribution in units of σ

These two trends, the increase in stress as the probe size approaches the pore size and then a drop in the observed stress when the probe size surpasses the pore size, lead to a maximum in the

bending stress when the probe molecule is close to the average pore size. In Figure 3 it is clear that the maximum bending stress is seen when probe size is equal to the solvent from which the film was deposited.

CONCLUSION

The effect of solvation stress on a microporous thin film is an extremely sensitive measure of adsorption. Using both the kinetics and the magnitude of the change in solvation stress as a result of a change in overlying vapor pressure of a solvent, we have measured the accessibility of various alcohols into microporous sol-gel thin films. As the probe size approaches the characteristic pore or constriction size, the rate of change in the stress induced in the film is reduced. As the probe size is further increased in relation to the pore size, the magnitude of the stress change drops because less of the pore volume is accessible. We see that gels prepared with pendant phenyl groups, have a larger final pore size than gels prepared with standard tetrafunctional alkoxides. By replacing the solvent from which the film was deposited we see that the characteristic pore size in these acid catalyzed sol gel films is a result of the inorganic network collapsing and templating around the solvent molecules. This method of solvent templating allows relatively facile manipulation of the pore size in the <1 nm range.

ACKNOWLEDGMENTS

The authors thank Rich Cairncross for helpful discussions and Hongbin Yan and Thomas M. Niemczyk for the IR measurements. This work was supported by the U.S. Department of Energy Basic Energy Sciences Program, the University of New Mexico/National Science Foundation Center for Micro-Engineered Ceramics and the National Science Foundation Division of Chemical and Transport Systems (CTS9101658). Sandia National Laboratories is a U.S. DOE facility operated under contract number DE-AC04-94AL 85000.

REFERENCES

1. N.K. Raman, C. J. Brinker; J. Membrane. Sci. **105**, 273 (1995).
2. P.Behrens; Adv. Mater. **5**, 19, (1993) .
3. S.J. Gregg, K.S.W Sing ; Adsorption, Surface Area and Porosity (Academic Press 1982).
4. T.J. Bandosz, J. Jagiello, K. Putyera, J.A. Schwarz; Langmuir **11**, 3964 (1995).
5. A.J. Ricco, G.C. Frye, S.J. Martin; Langmuir **5**, 273 (1989).
6. J. Samuel, unpublished data.
7. M.A. Fadad, E.M. Yeatmen, E.J.C., Dawnay, M. Green, F. Horowitz; J. Non. Cryst. Sol. **183**, 269 (1995).
8. E.M. Corcoran; Journal of Paint Technology **4**, 635 (1969).
9. J.H.L.Voncken, C. Lijzenga, K.P.Kumar, K. Keizer, A.J. Burggraaf, B.C. Bonekamp; J. Mat. Sci. **27**, 472-478 (1992).
10. G.W. Scherer, D.M.Smith ; J. Non Cryst Solids **189** (1995).
11. C.G.V. Burgess, D.H. Everett; J. Colloid. Interface Sci. **33**, 611 (1970).
12. R.A.Cairncross, P.R Schunk, K.S. Chen, S.S. Prakash, J. Samuel, A.J. Hurd, C.J. Brinker; Proceedings of the Society for Imaging Science and Techology (1996).
13. C.J. Brinker, G.W Scherer; SOL-GEL SCIENCE, (Academic Press 1990).
14. S.K.Garg, A. Nur ; J.Geophysical Research **78**, 5911-5921(1973).
15. O.Kadlec, M.M. Dubinin; J. Colloid Interface Sci. **31**, 479 (1969).
16. J Klein, E Kumacheva; Science, **169**, 816 (1995).

DISCLAIMER